Organic Process Research & Development

Article

pubs.acs.org/OPRD

Rapid Crystallization Process Development Strategy from Lab to Industrial Scale with PAT Tools in Skid Configuration

Somnath S. Kadam,*[,†] Jochem A. W. Vissers,[‡] Marco Forgione,[§] Rob M. Geertman,[¶] Peter J. Daudey,[∥] Andrzej I. Stankiewicz,[†] and Herman J. M. Kramer[†]

[†]Intensified Reaction & Separation Systems, Process and Energy Laboratory, Delft University of Technology, 2628 CA Delft, The Netherlands

[‡]Control Systems group, Department of Electrical Engineering, Eindhoven University of Technology, 5600 MB Eindhoven, The Netherlands

[§]Delft Centre for Systems and Control, Delft University of Technology, 2628 CD Delft, The Netherlands

[¶]Solid State Chemistry, API Process Development, Merck Sharp and Dohme, 5342CC Oss, The Netherlands

[∥]Albemarle Catalysts Company B.V., Nieuwendammerkade 1-3, 1030 BE Amsterdam, The Netherlands.

ABSTRACT: Batch cooling crystallization is a commonly used separation and purification step in the pharmaceutical industry. Various properties of the crystalline product from a batch crystallizer can have a strong impact on the efficiency of downstream processes such as filtration and drying, on the formulation process and on the dissolution behaviour of the drug. Development of the crystallization processes presents a major challenge in the process development of an active pharmaceutical ingredient (API). Therefore, it is beneficial to develop a rapid crystallization process development strategy to industrial scale. In this paper we present a strategy for rapid process development and apply this strategy for androsta-1,4-diene-3,17-dione, cyclic 17-(2,2-dimethyltrimethylene acetal), a pharmaceutical intermediate produced by Merck Sharp and Dohme. The major advantages of the strategy are that there is no requirement of the crystallizer design modification, the calibration of the process analytical technology (PAT) tools can be performed at industrial scale, and the determination of the operating window can be done directly at the industrial scale. This strategy allows for process optimization directly at the industrial scale, thus eliminating the need for time-intensive scale-dependent study. The implementation of this strategy at industrial scale was performed with the help of PAT tools arranged in a unique skid-based configuration. The skid which contains both the concentration sensors and the crystal size distribution (CSD) sensors can be connected to the existing crystallizers, thereby avoiding the time and cost-intensive modifications in the crystallizer design. The modular nature of the skid offers opportunities to choose the PAT tools which complement the solute−solvent model system. The skid makes it possible to gather the relevant information concerning the thermodynamics and kinetics of the model system in situ during the crystallization runs at the industrial scale. A strategy for process development based on a sensor skid is beneficial for the industry as it is intrinsically rapid and can be combined with the development of control strategies which lead to consistent product quality.

1. INTRODUCTION

Batch cooling crystallization is a commonly used separation and purification step in pharmaceutical industry as it is easy to operate, less energy intensive, can achieve high purity in a single step, etc.[1] Although batch cooling crystallization has several advantages, batch-to-batch variations in crystalline product quality are commonly observed which have a strong impact on the product properties such as flowability, agglomeration tendency, tableting, and dissolution behaviour, etc. Inconsistent product quality can also affect the efficiency of the downstream processes such as drying and milling.[1] Due to its critical role in the production process, crystallization presents a significant process development challenge when a new drug is to be synthesized commercially.

Attempts have been made in the past to develop crystallization strategies which are applicable to the existing crystallizers.[2−4] Typical steps involved in such a process development strategy and its current limitations are schematically represented in Figure 1.

The steps in process development can be divided into three parts, lab scale, pilot-plant scale, and industrial scale. The scale-dependent study during the conventional process development process is performed as the micromixing, macromixing and heat transfer effects vary with the scale. This leads to variable temperature and supersaturation profiles and hence variable crystallization kinetics. By scale-dependent study, the amount of variation in the crystallization kinetics can be determined.[5]

The first set of experiments at lab scale is devoted to determine a solvent (Figure 1, block a). This set of experiments consists of interrelated steps for solvent screening, polymorph screening, and determination of the method of supersaturation generation. The second set of experiments at lab scale is performed to determine the operation window for the process and the crystallization kinetics (Figure 1, block b). Once the solvent, operation window, and crystallization kinetics are determined, process development continues at industrial scale

Received: March 6, 2012
Published: April 20, 2012

dx.doi.org/10.1021/op300055g | *Org. Process Res. Dev.* 2012, 16, 769−780

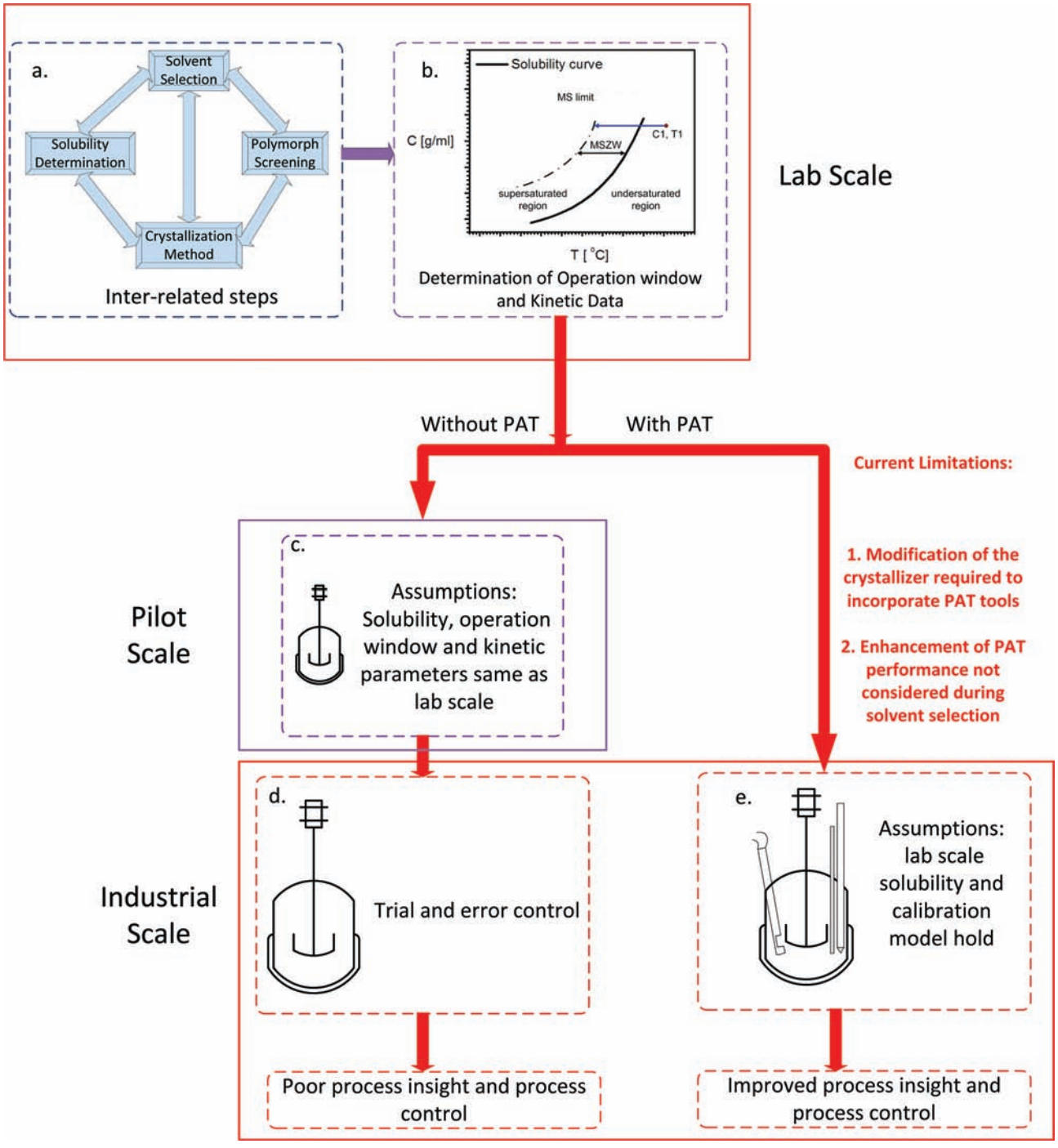

Figure 1. Typical process development strategies from lab to industrial scale with and without process analytical technology (PAT) along with their limitations.

through a pilot plant (Figure 1, blocks c and d) when performed without PAT tools and without a pilot plant when performed with PAT tools (Figure 1, block e). When PAT tools are available, process optimization becomes possible at the industrial scale directly, which eliminates the need of scale-dependent study. The details of the steps involved are described in sections 1.1.1 to 1.1.3.

1.1. Lab Scale. *1.1.1. Solvent Screening and Method of Supersaturation Generation.* The process development usually starts with solvent screening. For a cooling crystallization process, a solvent with a solubility that increases enough to yield approximately 10−20% solids over a reasonable cooling trajectory is desirable. If the dependency of the solute solubility on temperature is not adequate, other methods of supersaturation generation such as evaporation, antisolvent addition, or a combination of different methods can be employed.[6] Solvent screening can be completely or only partially based on experiments. For the complete experimental approach, the solubility of the solute is determined in a wide variety of commonly used industrial solvents at room temperature. For solvents which display good solvation (between 5 and 200 mg/mL), the solubility is also determined at higher temperatures.[2] For the other approach, an initial solvent screening is performed with models such as

dx.doi.org/10.1021/op300055g | *Org. Process Res. Dev.* 2012, 16, 769−780

UNIQUAC, COSMO-RS, NRTL-SAC, etc. which can predict temperature-dependent solubility of chemicals in different solvents.[7−10] On the basis of the predicted yield by these models, a few solvents can be selected, the solubilities of which are experimentally determined as a function of temperature. Other considerations such as the toxicity of the solvent and its environmental impact may also influence the choice of solvent.[2]

1.1.2. Polymorph Screening. Polymorph screening is necessary to identify the most stable polymorph and to verify that the most stable polymorph is obtained directly after the batch. Polymorphs encountered in the crystallization process depend on, amongst other factors, the solvent used. Solvent plays a crucial role in the polymorphic outcome of the crystallization process as it can promote or inhibit hydrogen bonding during formation of molecular clusters and hence control the nucleation of a specific solid form.[11,12] There are several methods of polymorph screening[13] which vary in their effectiveness of screening and the time required for their implementation. Slurry testing is one of the commonly employed methods as it is very effective in identifying low-energy polymorphs and also in identifying solvates.[11,14]

On the basis of the outcome of solvent screening, polymorph screening, and temperature-dependent solubility measurements, a solvent is selected for the crystallization process.

1.1.3. Determination of the Operation Window and the Crystallization Kinetics. The metastable zone width (MSZW) can be considered as the preferred operating region in the composition−temperature space. It forms the area between the solubility curve and the MSZ limit at which the crystals are detected at a constant cooling rate.[1] A polythermal method[15] is commonly used for determining MSZW during cooling crystallization.

Along with the MSZW, the polythermal method can also be used for determining nucleation kinetics.[16] The other common methods for determining nucleation kinetics are the induction time measurement method[17,18] and the double pulse method.[19] Crystal growth rates can be determined by following the time evolution of a particular face of a crystal in stagnant solution with time,[20] by using the mixed slurry mixed product removal (MSMPR) crystallization experiments in combination with the population balance equations,[6] by following crystal size distribution (CSD) in time,[21] by combining the crystal shape evolution model with the population balance model,[22] or by using indirect methods such as following the desupersaturation curve after seeding with a known amount of seeds.[23] It is beneficial to use the PAT tools for determination of the crystallization kinetics as it releases the requirement for sampling, thus allowing the measurements to be automated and resulting in a sufficient amount of information on crystallization behaviour of the model system in a short amount of time. However, PAT tools which deliver accurate measurement of process variables are scarce.

On the basis of the determined kinetic data at lab scale, an optimal or a near optimal cooling profile which could be implemented during crystallization at industrial scale can be determined.[24] The use of PAT tools at lab scale also enables implementation of interesting strategies within the operating window such as temperature cycling which could allow control over polymorphic purity.[25]

1.2. Pilot and Industrial Scale. Depending on the accessibility, the crystallization process at industrial scale can be performed with or without PAT tools.

1.2.1. Process Development without PAT. As PAT tools are expensive and their implementation in an industrial-scale crystallizer might require substantial changes in the design of the crystallizer, the most common approach is to continue with the process development at industrial scale without PAT (Figure 1 block d) through a pilot-plant stage (Figure 1 block c). Following this approach it is assumed that the solubility, MSZW, and kinetic models determined at lab scale remain valid at the pilot-plant and industrial scale. Seeding is commonly employed at industrial scale to start the crystallization process.[6] After seeding, a cooling profile which is predetermined offline is often followed to maintain the same level of supersaturation throughout the process.[1] This cooling profile is determined on the basis of the lab-scale MSZW and the crystallization kinetics. During the implementation of the cooling profile, the crystal product quality evolution is not monitored, and it is assumed that the product quality obtained would be similar to that at lab scale. However, the performance at pilot-plant and industrial scale does not often match the performance at lab scale when this approach is implemented. This is primarily due to lack of scale-up rules and inhomogeneous mixing giving rise to areas of nonuniform energy dissipation and temperatures and supersaturation.[5,26] The effect of inhomogeneous mixing on crystallization kinetics will vary from one model system to other. The use of a pilot plant can give an estimate for the amount of deviation from the expected product quality due to inhomogeneous mixing at larger volumes. Taking corrective measures at pilot scale or industrial scale would require redetermination of kinetic parameters or operating procedures. This approach of scale-up without PAT is based on trial and error, and poor process insight is often the result of this approach. Sampling and offline analysis could provide some insights in the process, but the insights are not enough to develop rigorous control strategies.

1.2.2. Process Development with PAT. The process development with PAT tools offers a better opportunity to obtain consistent product quality. The use of PAT tools allows for the monitoring of crystal quality in real time. Process monitoring can be combined with process modelling and estimation tools to obtain kinetic parameters in situ at industrial scale. This enables designing of the control strategies[27−29] with minimum *a priori* knowledge and capabilities to learn from batch-to-batch.

However, the implementation of PAT tools at industrial scale currently requires time and cost-intensive modifications in the design of the crystallizer.

2. INCENTIVE FOR THE WORK

In the current approach of process development to industrial scale there are the following limitations:

(1) Process development without PAT is based on the assumption that the solubility, MSZW, and the kinetic parameters determined at lab scale also hold at pilot and industrial scale. This approach ignores the fact that the MSZW is scale-dependent,[30] the impurity profile may be different at industrial scale, and inhomogeneous mixing may lead to areas of variable supersaturation at pilot and industrial scale.

(2) Process development to industrial scale with PAT requires several modifications in the design of the crystallizer to incorporate the PAT tools. The incorporated PAT tools are calibrated at lab scale and used at

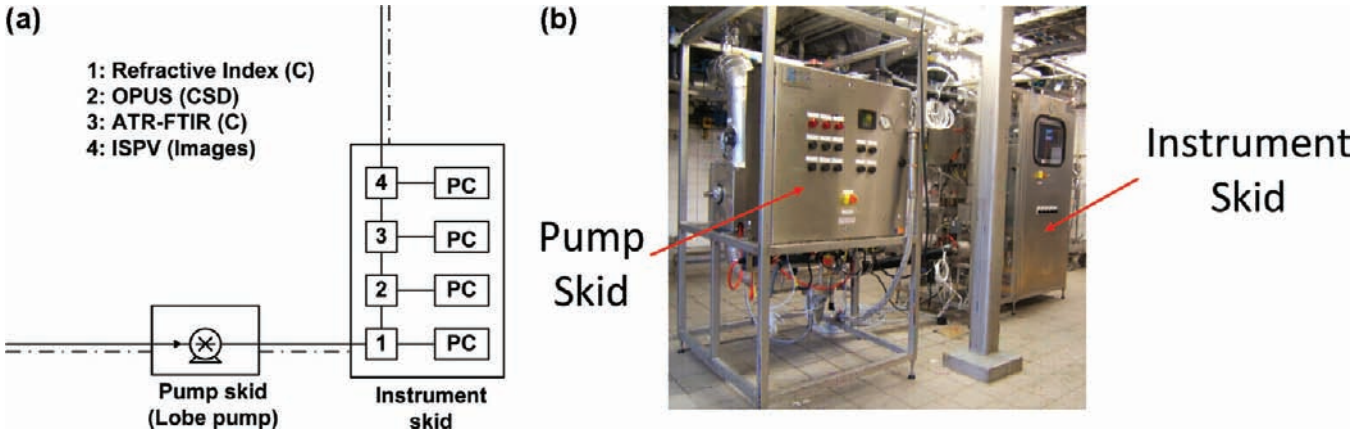

Figure 2. (a) Schematics of the pump and the instrument skid. (b) The pump and the instrument skid

industrial scale. This approach results in time and cost-intensive modifications of the industrial crystallizer and also leads to biased measurements as the calibration models are not developed at industrial scale.

In this paper we present a rapid strategy for process development with PAT tools in a unique skid-based configuration which addresses the above-mentioned limitations in the shortest possible time. This strategy for process development does not make assumptions about the solubility and the kinetic parameters being constant at lab and industrial scales, does not need major modifications in the design of the vessel, and allows direct calibration of the concentration measuring instruments at industrial scale. The process development strategy is demonstrated for androsta-1,4-diene-3,17-dione, cyclic 17-(2,2-dimethyltrimethylene acetal). The process development part at lab scale was performed at Merck Sharp and Dohme, Oss, The Netherlands, while the industrial part was performed at Merck Sharp and Dohme, Apeldoorn, The Netherlands.

3. SKID DESIGN AND ITS ADVANTAGES

In order to overcome the limitations mentioned in section 2, Incentive for the Work, the PAT tools were arranged in a unique skid-based configuration as shown in Figure 2. The skid was manufactured by Zeton B.V. (The Netherlands).

The configuration consisted of two skids, viz. the instrument skid and the pump skid

3.1. Instrument Skid. The instrument skid consisted of a stainless steel pipeline with an internal diameter of 2.54 cm for the flow of the slurry and four PAT tools and their computers enclosed in a pressurized cabinet as shown in a and b of Figure 2. The PAT tools used in the skid are listed in Table 1.

The details of the working principles and the performances of the sensors listed in Table 1 are available in the literature.[31−34] The BRIX sensor was installed at an angle of 45° to the flow to allow for the self-cleaning effect of the prism. The OPUS, ATR-FTIR, and ISPV were installed perpendicular to the flow with the measuring sections of the instrument coinciding with the centre of the flow. The interferometer of the ATR-FTIR was flushed continuously with nitrogen gas to avoid the effect of atmospheric carbon dioxide and water vapour on the collected spectra. The ISPV sensor consisted of a set of two video microscopes with the resolutions of 10 μm/pixel (low resolution) and 2 μm/pixel (high resolution). Imaging can in principle be used to determine CSD during the process. During this work, imaging was used in a qualitative manner to gain process insights. Hence, CSD has been included in brackets in Table 1 for the ISPV. OPUS was included in the skid for CSD measurements but was not used during the experiments as it needs *a priori* calibration which was not performed for ADD-NEOP. The computers of the PAT tools were placed in the slightly pressurised skid cabinet along with the controller computer and software from IPCOS (The Netherlands). The controller software could interact with the control system of the crystallizer. The instrument skid was also equipped with a display screen on which measurement trends from individual PAT tools and from the IPCOS controller could be seen in real time.

Table 1. PAT tools in the skid to monitor concentration (C) and crystal size distribution (CSD)

PAT tool (model name)	supplier	measured property	monitored variable
BRIX sensor/process refractometer (PR-23-IA)	K-Patents (Finland)	refractive index of the solution	C
OPUS	Sympatec (Germany)	ultrasound attenuation	CSD
ATR-FTIR[a] (MATRIX-MF)	Bruker Optics (Germany)	absorption of the infrared radiations	C
ISPV	Perdix Analytical Systems	(images)	(CSD)

[a]ATR-FTIR: attenuated total reflectance - Fourier transform infrared spectroscopy.

The instrument skid was connected to the pump skid and the crystallizer with the help of traced flexible hoses.

3.2. Pump Skid. The pump skid consisted of a lobe pump (BF 330, OMAC, Italy) placed in the pressurized cabinet. The pump consisted of two lobes rotating in the direction opposite to each other. When the lobes moved away from each other, the slurry or solution flowed into the rotor case which was then discharged on the opposite side when the lobes moved towards each other. The inlet and outlet openings of the pump were 3″ in diameter, and the maximum flow-rate was approximately 120 L/min. The pump skid was connected to the instrument skid and the crystallizer with traced flexible hoses.

3.3. Advantages of the Skid Design. The configuration of the PAT tools in form of the skid leads to the following advantages

dx.doi.org/10.1021/op300055g | Org. Process Res. Dev. 2012, 16, 769−780

(a) The modification of the crystallizer is not required in order to connect the PAT tools. This saves valuable industrial time and also the cost which would have been necessary for the design modification.
(b) The skid-based design allows for the easy transportation of the skid from one location to the other.
(c) The skid is modular in nature allowing for the addition or removal of the PAT tools as per requirements.
(d) Good flow conditions through the skid ensures that the measurements by the PAT tool are representative of the conditions in the crystallizer.

4. EXPERIMENTAL SECTION

Experiments were performed with androsta-1,4-diene-3,17-dione, cyclic 17-(2,2-dimethyltrimethylene acetal) (Dutch name: androstadieen-3,17-Dion-17-Neopentylketaal, acronym: ADD-NEOP) as a solute. ADD-NEOP (Figure 3) is a pharmaceutical intermediate synthesized by Merck Sharp and Dohme, The Netherlands, and was used without further purification.

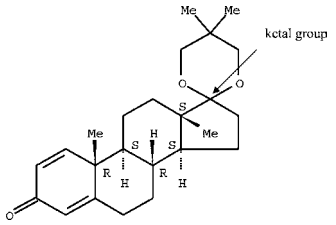

Figure 3. ADD-NEOP absolute stereochemistry[35].

ADD-NEOP consists of a ketal group which hydrolyzes in presence of acidic environment. Hence, a small amount (0.5% v/v) of base (triethyl amine, TEA, analysis grade, J.T. Baker) is added to stabilize ADD-NEOP solution when used in acidic environment.

4.1. Solubility Measurements. Initial solvent screening was performed for 50 commonly used industrial solvents with COSMO-RS.[9] On the basis of the differences in solubility of ADD-NEOP in these solvents predicted by COSMO-RS between 50 and 20 °C, four solvents were chosen. The solubility measurements were performed in these four solvents which were all analysis grade procured from J.T. Baker. For acidic solvents 0.5% v/v of TEA was added to protect the ADD-NEOP molecule from hydrolysis. The solubility measurements were performed using a multiple reactor setup (Crystal16, Avantium Technologies). The setup consisted of 16 magnetically stirred 1 mL vials in which transmission of light through the solution was recorded. Slurries with different concentrations were prepared in the vials and were stirred at 700 rpm. The heating and cooling rates employed were 0.5 °C/min. Upon heating a vial in the setup, the transmission of the light through the solution became 100% at a certain temperature. That temperature was taken as the saturation temperature of that sample. The heating and cooling cycles were repeated at least four times per concentration to have a better estimate of the solubility.

4.2. Slurry Test. Slurry tests were performed at room temperature to identify the most stable polymorph appearing from the four solvents chosen in section 4.1, Solubility Measurements. Slurries were prepared with approximately 1000 mg of ADD-NEOP in 5 mL of each of the four solvents. They were stirred on IKA Ret basic stirring plates for 26 days continuously to allow any metastable polymorphic form to transform into a stable polymorphic form. After the end of the 26th day, the slurries were vacuum filtered through VitraPOR sintered glass filter (Gereate GmbH, Germany) with pore size of 16−40 μm. The filtered slurries were vacuum-dried at 8 mbar for 48 h and were analyzed by X-ray powder diffraction (XRPD). Batch cooling experiments between 40 and 20 °C were also performed at 5 mL scale in all four solvents in order to verify that the stable polymorph was obtained directly at the end of the batch.

4.3. Infrared Spectra Collection. The relative positions of ADD-NEOP peaks and solvent peaks were introduced as the new criteria for solvent selection which would enhance the performance of the ATR-FTIR spectroscopy. The details of motivation behind introduction of these criteria are mentioned in section 5.3, Infrared Spectra. Undersaturated solutions (25% w/w of the saturation concentration) were prepared in four solvents at room temperature. Mid-infrared (MIR) spectra were collected in ATR mode with ReactIR45m (Mettler-Toledo) with resolution of 8 cm^{-1} in the range of 2800−650 cm^{-1}. Each spectrum consisted of 256 coadded scans. A background spectrum was collected in air at room temperature. Collection of background spectra in air was preferred over collection in solvent as the solvent spectra are very sensitive to minute changes in temperature.[21]

4.4. Combined Characterization and PAT Tool Selection at Lab Scale. The operating region, i.e. the MSZW, is commonly determined on the lab scale without much consideration of the volume at which experiments are performed. Experiments at small volumes lead to distribution of MSZW, while as the volume is increased, the MSZW becomes reproducible within a small error margin.[30] Hence, care must be taken to determine MSZW at sufficiently large volumes at which it is reproducible. The MSZW measurements can be combined with the identification of the PAT tool which works better for the model system under consideration. A given PAT tool will have different accuracy when used with different model systems,[33] and also different PAT tools used for the same model system will have different accuracies.[36] Hence, identifying the PAT tools which best suits the model system at lab scale itself will improve process monitoring at industrial scale.

The two steps mentioned above, i.e. determination of the MSZW and selection of PAT tool, can be combined together to make the process development rapid. In order to do so, experiments were performed in a 2 L baffled jacketed glass crystallizer which was agitated by an anchor type impeller at 175 rpm to determine MSZW for ADD-NEOP in the solvent selected on the basis of experiments in sections 4.1 to 4.3. The concentration of ADD-NEOP was 173 mg/mL which had a saturation temperature of 41.4 °C. The cooling was performed linearly at a cooling rate of 0.5 °C/min. The experiments were monitored by visual observation, focused beam reflectance measurements (FBRM) (Mettler-Toledo), and an in situ particle viewer (ISPV) (Perdix Analytical Systems). The measurement was performed by FBRM every 10 s, while images were taken by ISPV every second. The ISPV had a resolution of 1 μm/pixel. The experiment was performed twice to check the reproducibility of the MSZW measurements.

4.5. Combined Calibration and Characterization at Industrial Scale. Calibration models for the PAT tools which are developed at lab scale may not necessarily work at industrial

dx.doi.org/10.1021/op300055g | Org. Process Res. Dev. 2012, 16, 769−780

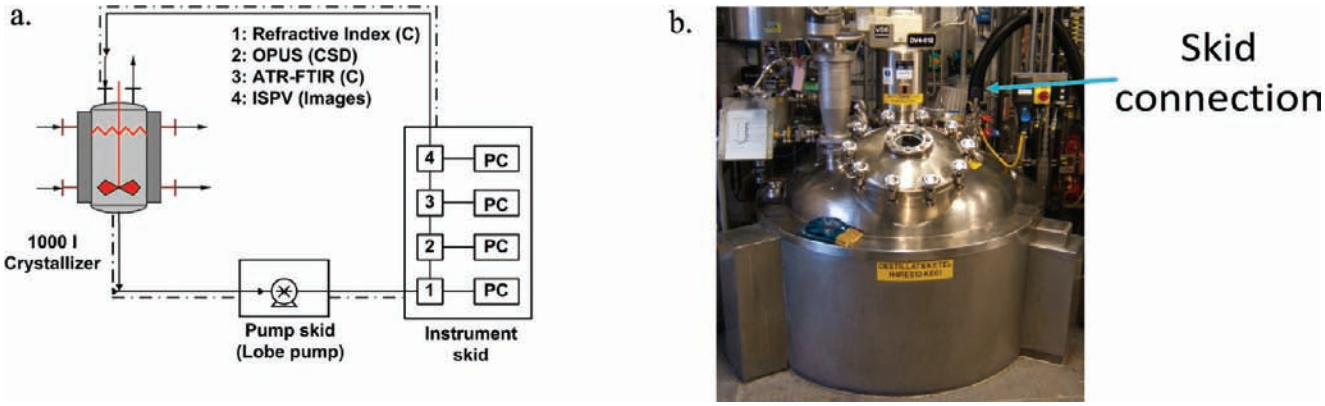

Figure 4. (a) Schematics of the instrument skid and pump skid connected to the crystallizer. (b) Inlet connection to the crystallizer from the skid.

scale. Especially the attenuated total reflectance Fourier transform infrared spectroscopy (ATR-FTIR) which is used for concentration measurements is sensitive to minute changes in the operating environment.[21] Hence, it is beneficial to perform calibration directly at industrial scale. The calibration of the PAT tools can be combined with process characterization at industrial scale to rapidly develop the process. The time- and cost-intensive steps of modifying the design of the crystallizer to incorporate PAT tools can be avoided by using the instruments in the form of a skid as shown in Figure 4. The instrument skid can be connected to the crystallizer with help of a pump skid and flexible hoses. There are often inlet and outlet connections already in the original design of the crystallizer, and hence, the modification of the vessel is not necessary.

The industrial-scale experiments reported here were performed at Merck Sharp and Dohme, Apeldoorn, The Netherlands. The crystallizer used for the experiments (Figure 4b) was a 1000 L jacketed stainless steel vessel equipped with a vacuum system and a condenser. The stirring was performed at 125 rpm with the help of a three-blade propeller. The crystallizer was connected to the pump skid and the instrument skid with help of traced insulated flexible hoses.

Figure 5 shows the schematics of the combined calibration and characterization step; 904.5 L of solvent was added to the crystallizer at 5 °C. The background scan for ATR-FTIR was collected in air before the pumping of the solvent through the skid was started. ADD-NEOP (43.74 kg) was added to the crystallizer through the manhole. Vacuum was applied on the crystallizer to vaporize ethanol which was condensed and drained along the walls of the crystallizer to remove any ADD-NEOP sticking on the crystallizer wall. The crystallizer environment was made inert by purging in nitrogen gas, and the slurry was heated at 0.3 °C/min. The spectra for ATR-FTIR and the BRIX readings were collected continuously. Slow heating allowed for the determination of the saturation temperature at the given concentration and hence for determination of one side of the operation window. The crystallizer was maintained 5 °C above the saturation temperature for 30 min and then cooling was started at 0.4 °C/min to 5 °C. During the cooling process the onset of crystallization or the metastable limit which forms the other side of the operation window was determined. Cooling was always performed to 5 °C (which is below the flash point of solvent) so that the next batch of the ADD-NEOP can be added by opening the manhole of the crystallizer. The process of heating and cooling was repeated four times by adding loads of 27.4 kg each.

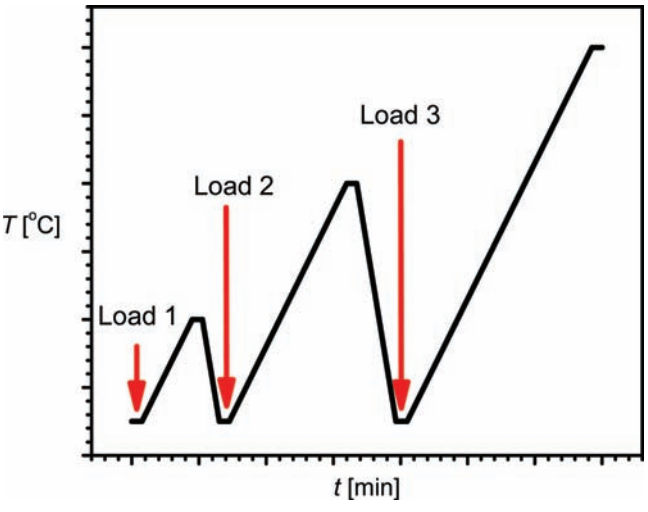

Figure 5. Schematics of the combined calibration and characterization step.

4.6. Gaining Process Insights. In situ imaging has been shown previously to provide valuable process insights.[30] In this contribution, in situ imaging was used to monitor the initial phases of an unseeded and seeded batch crystallization process in order to gain insights about secondary nucleation. For unseeded batch cooling crystallization, the crystallizer at 50 °C containing solution saturated at 40 °C was cooled to 36 °C linearly at the rate of 0.5 °C/min. The crystallizer was maintained at 36 °C for 1800 s, and images were collected with both the high- and low-resolution cameras at an interval of 2 s in order to check if crystals appear within 1800 s. The crystallizer was then heated back to 50 °C and was maintained at 50 °C for an hour in order to make sure that the solution was free from any crystalline material. Vacuum was applied in the crystallizer to evaporate part of the solvent which was then condensed and drained on the walls of the crystallizer to make sure that no crystalline material was sticking on the wall. The crystallizer was brought to 36 °C at 0.5 °C/min cooling rate and was seeded with a single seed crystal as shown in Figure 6 which was approximately 10 mm in length, 2 mm in height, and 2 mm in breadth.

dx.doi.org/10.1021/op300055g | Org. Process Res. Dev. 2012, 16, 769−780

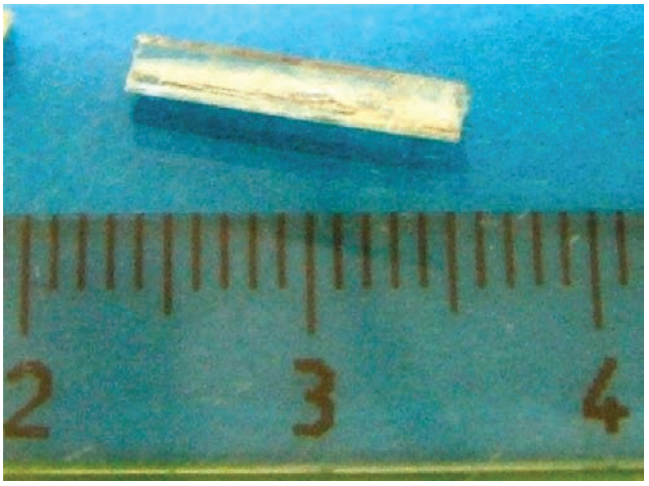

Figure 6. Single crystal used for seeding.

The single crystal was prepared by slow evaporation of solvent. The resulting evolution of the crystal number was followed with the help of in situ imaging.

5. RESULTS

5.1. Solubility Measurements. Of the 50 commonly used industrial solvents which were screened with COSMO-RS for solubility predictions, ethanol, propanol, ethyl acetate, and acetone were selected on the basis of the difference in solubilities at 50 and 20 °C. As ethanol and propanol are slightly acidic, 0.5% v/v of triethyl amine (TEA) was added to them to prevent hydrolysis of ADD-NEOP. The solvent names (ethanol and propanol) are used henceforth in this paper without mentioning the name of the base. A solvent which would lead to 10% solids when the crystallization process is operated between 40 and 10 °C was to be identified on the basis of the solubility measurements. The temperature window between 40 °C−10 °C and the solid concentration of 10% leads to an economically favorable operation of the chosen crystallizer based on the experience of the staff and was chosen without further investigation.

As can be seen from Figure 7, the solubility of ADD-NEOP in ethyl acetate rises very steeply, making it the least attractive

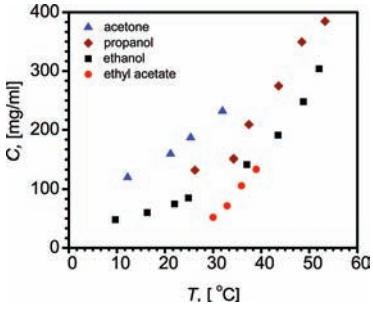

Figure 7. Temperature-dependent solubilities of ADD-NEOP in acetone, propanol, ethanol, and ethyl acetate.

of the solvents under consideration as the solids content would be more than 10% at the end of the batch when operated between 40 and 10 °C. For acetone, propanol, and ethanol the steepness of the solubility curve between 40 and 10 °C is approximately the same and would lead to 10% solid concentration at the end of the batch. On the basis of the solubility criteria any of the solvents from acetone, propanol, and ethanol could be used.

5.2. Slurry Test. The slurry test was performed to identify the most stable polymorph in the solvents under consideration. XRPD patterns of the crystals obtained after the slurry test are shown in Figure 8.

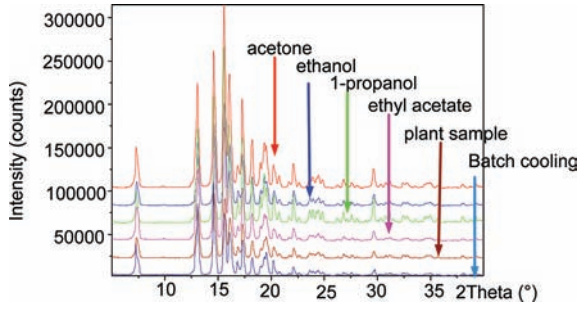

Figure 8. The XRPD patterns after the slurry tests and the batch cooling experiment in ethanol. The same stable polymorph is obtained from all the solvents and after the batch cooling experiment.

As can be seen from Figure 8, the same stable polymorph was obtained from all the solvents. Also the ADD-NEOP which was supplied for the experiments from the plant was also in form of the stable polymorph. Batch cooling experiments at 5 mL scale in all the solvents also resulted directly in the stable polymorph. On the basis of the polymorphic outcome, all four solvents are found suitable for use.

5.3. Infrared Spectra. ATR-FTIR spectroscopy is one of the most suitable and commonly used technique for monitoring concentration during crystallization processes.[33,37] A multivariate calibration method is often used for obtaining concentration values based on the measured spectra.[38] The multivariate approach considers the intensity differences as a function of wavenumbers within the spectrum taken at a particular process condition and also the intensity differences between different spectra at a particular wavenumber taken during the changes in process conditions.[39] The change in concentration of the solute during the crystallization process would predominantly be seen as changes in peak height and width of the solute peak. Performing multivariate calibrations in the region around the solute peak would increase the chance of developing a calibration model with high accuracy and low rank.[38]

The performance of the ATR-FTIR spectroscopy could be enhanced if the solute peak is distinct from the solvent peaks. Hence, the IR spectrum could be used as a criterion for solvent selection.

As can be seen from a and d of Figure 9, respectively, the mid-infrared spectrum of ADD-NEOP in acetone and ethyl acetate do not show distinct solute peaks. A small shoulder due to the ADD-NEOP carbonyl stretch is present (around 1700 cm^{-1}) on the peak due to the carbonyl stretch of the solvent. On the other hand for ADD-NEOP in ethanol and propanol a distinct carbonyl peak is seen which makes them both attractive solvents. As the solubility of ADD-NEOP in ethanol is less than in propanol, ethanol was selected as the solvent for further experiments.

5.4. Combined Characterization and PAT Tool Selection at Lab Scale. The MSZ limit, which determines one side of the operation window, was determined for 173 mg/mL of ADD-NEOP in ethanol with help of visual observations,

dx.doi.org/10.1021/op300055g | Org. Process Res. Dev. 2012, 16, 769−780

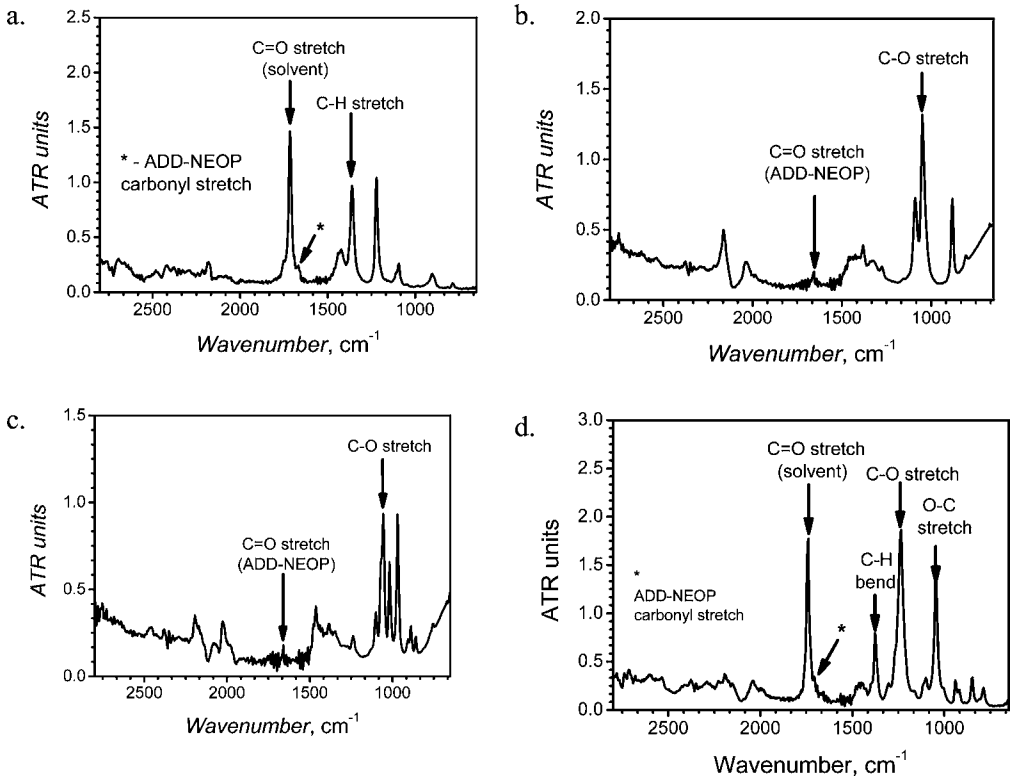

Figure 9. Mid-infrared spectra of ADD-NEOP in acetone (a), ethanol (b), propanol (c), and ethyl acetate (d).

ISPV and FBRM at 2 L scale with a cooling rate of 0.5 °C/min. As can be seen from Figure 10, ISPV detected the particles

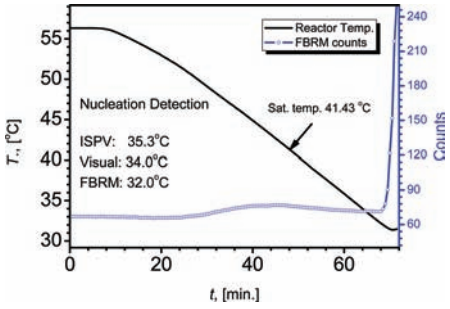

Figure 10. MSZW measurement with different PAT tools.

almost 3 °C (6 min) prior to FBRM and almost 1.5 °C (3 min) prior to visual observations. The ISPV detects particles before FBRM as the measurement volume of ISPV is larger than that of the FBRM. FBRM relies on detection of crystals based on a laser beam which requires certain minimum crystal volume fraction. When the crystallization kinetics are faster, a certain minimum crystal volume fraction required for FBRM for particle detection can be attained faster. For such systems, ISPV and FBRM might have comparable performance in detecting particles.

The experiment above for MSZW measurement was repeated again, and the MSZ limit was reproducible within 0.3 °C. The smallest MSZW was measured by ISPV and was 6.1 °C. As ISPV was more sensitive in detecting particles, it was decided to use it at industrial scale for detecting particles. The MSZW measurements can also be used for kinetic parameter estimation and determination of batch recipe.[40,41]

5.5. Combined Calibration and Characterization at Industrial Scale. *5.5.1. Calibration.* For the calibration of ATR-FTIR and BRIX sensor, concentrations and temperature ranges used are shown in Table 2.

Table 2. Concentration and temperature ranges used for calibration of ATR-FTIR and BRIX sensor

		temperature range [°C]	
concentration [mg/mL]	saturation temperature [°C]	upper temperature	lower temperature
48.3	10.0	15.0	5.0
78.6	22.5	29.0	17.5
108.9	30.0	34.5	25.0
139.3	35.5	41.5	30.0
169.6	39.8	45.2	34.7

Collection of spectra and BRIX values was carried out as described in section 4.5, Combined Calibration and Characterization at Industrial Scale. For calibration of ATR-FTIR spectroscopy the region between 1816.9 cm^{-1} and 794.7 cm^{-1} was used, and the first derivative was used as the preprocessing step. The details of the calibration for ATR-FTIR spectroscopy and different spectral preprocessing steps can be found in the literature[33] and are not described in details here. The root-mean-square error in prediction (RMSEP) for the calibration model was 0.521.

For the calibration of the BRIX sensor, a least-squares polynomial fit between the measured BRIX values was made with the known concentration values. The obtained polynomial is given as eq 1 and had a root-mean-square error of cross validation of 0.955.

$$C_{BRIX} = P_{00} + P_{10}B + P_{01}T + P_{20}B^2 + P_{11}BT \quad (1)$$

dx.doi.org/10.1021/op300055g | Org. Process Res. Dev. 2012, 16, 769−780

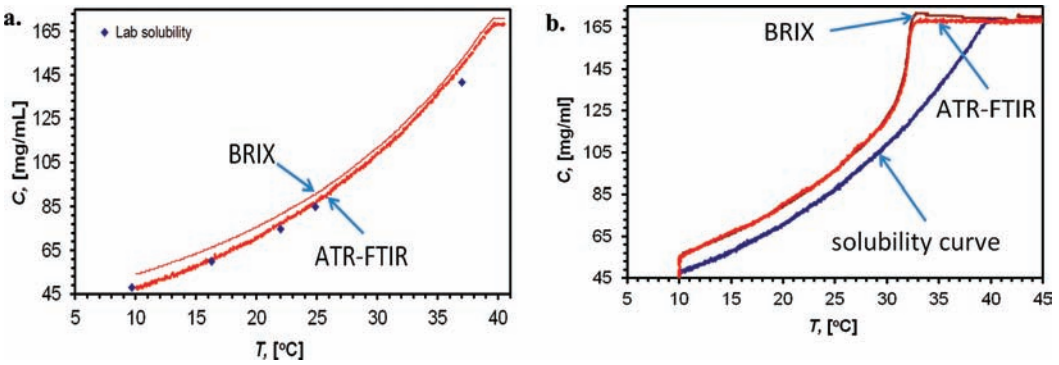

Figure 11. Process characterization at industrial scale: (a) solubility curve determined on industrial scale by ATR-FTIR and BRIX sensor, (b) the MSZW determined by ATR-FTIR and BRIX.

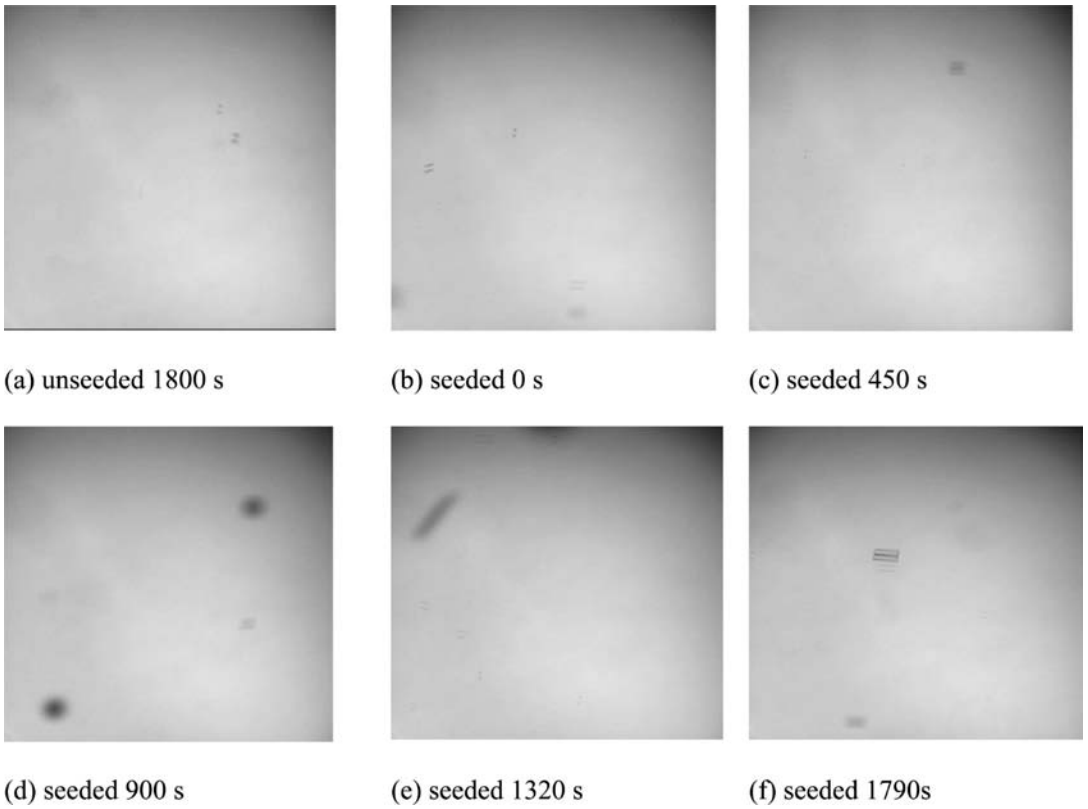

Figure 12. Images during the unseeded and seeded batch crystallization process by high-resolution camera.

where C is in mg/mL, T is in °C, and B represents BRIX values measured by the BRIX sensor. The obtained coefficients of eq 1 are

$$P = -139.5023, \quad P = 2.4562,$$
$$P = 0.3725, \quad P = 0.2819,$$
$$P = -0.0126$$

5.5.2. Characterization. The calibration procedure used here allows for characterization, i.e. determination of the operation window directly at industrial scale. The operation window at different concentrations is bound on one side by the solubility curve and on the other side by MSZ limit. As calibration is performed directly at industrial scale, the problems associated in concentration measurements due to minor misalignments of the hardware[21] are avoided. Also, as the solubility curve and MSZ limit are determined directly at the industrial scale, the effect due to impurities and the scale of experiments will already be accounted for.

Figure 9a shows the solubility measured with ATR-FTIR and BRIX sensor for ADD-NEOP in ethanol at industrial scale. The lab-scale solubility is plotted as a reference. As can be seen from Figure 11a, the solubility determined by ATR-FTIR agrees closely with the one measured at lab scale, while the solubility determined by BRIX sensor is higher than the lab-scale solubility. This is apparently due to the phase lag in the change of solution temperature and the change in the BRIX value associated with the temperature. The phase lag could be the result of the dynamics of the thermal path within the sensor and may be different while heating and cooling.. Coincidentally the solubility determined at lab scale agreed reasonably well with the solubility at industrial scale for ATR-FTIR. It might not be the case each time, and in those cases the concentration of the clear solution after dissolution of individual loads added

dx.doi.org/10.1021/op300055g | Org. Process Res. Dev. 2012, 16, 769−780

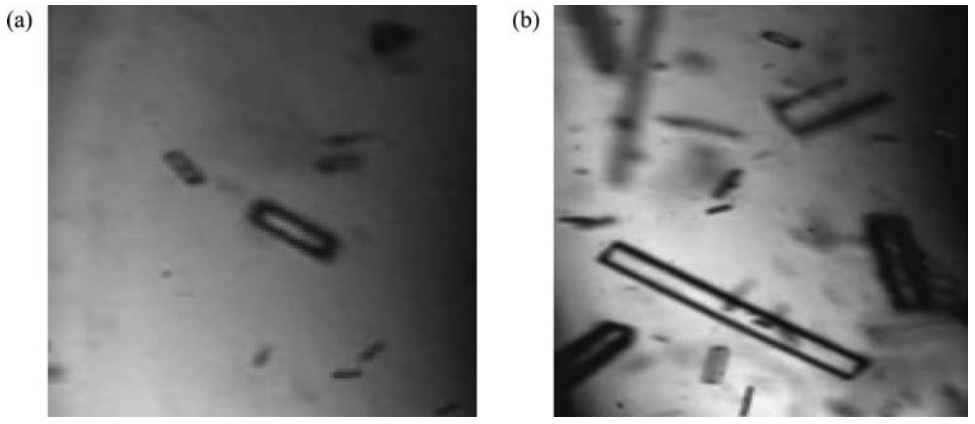

Figure 13. Crystals after 1790 s (a) and 2595 s (b).

during calibration could be used as a criteria. In this case, apart from the lab-scale solubility the measured value of concentration by ATR-FTIR agreed with the known value of concentration (amount of ADD-NEOP added to the solvent) at the end of the last load.

When the clear solution is cooled at a constant rate of 0.4 °C/min, the MSZ limit can be determined. The MSZ limit is reached when the drop in concentration occurs for concentration measurement PAT tools. For both the ATR-FTIR and BRIX sensor, the MSZ limit was reached at 33 °C, resulting in a MSZW of 6.8 °C. The larger MSZW, measured at industrial scale compared to lab scale, is probably caused by the different detection techniques. Surprisingly, after nucleation and growth of the crystals the concentration did not reach the solubility curve towards the end of the batch. This might be due to the effect of impurity incorporation within the crystals, but further research would be necessary before the exact cause could be determined.

5.6. Gaining Process Insights. The results obtained during the unseeded and seeded experiments are shown in the form of a series of images in Figure 12. All the images in Figure 12 were taken at 36 °C with a high-resolution camera in order to detect crystals as soon as possible. The time in the caption indicates the time elapsed after reaching 36 °C for an unseeded experiment, and for seeded experiments it indicates the time elapsed after seeding.

As can be seen from Figure 12 there were no crystals seen during the unseeded experiment for 1800 s, while for the seeded experiment with the single crystal, crystals started appearing around approximately 1000 s. The low-resolution camera gives a better indication of the amount of crystals as shown in Figure 13 as it has a higher depth of field.

Both the seeded and unseeded experiments can be considered to be performed under constant supersaturation. For the unseeded experiment, not a single crystal was spotted for the first 1800 s, while for the seeded experiment with a single crystal, crystallization was seen around 1800 s. This indicates that the crystals appearing in the seeded experiment are the result of secondary nucleation induced by a single crystal. Substantial crystallization around 2600 s as seen in Figure 13b suggests that a single crystal has the potential to act as a parent crystal and to lead to formation of the entire batch of crystals through secondary nucleation. As seen from a and b of Figure 13, under constant supersaturation of 1.25 the number of crystals formed due to secondary nucleation increases with time. Amongst other factors, the secondary nucleation rate is also proportional to the supersaturation.[42] Hence, in a constant cooling mode of operation during batch crystallization, the amount of crystals formed by secondary nucleation would increase with time and supersaturation. This indicates that there exists a subregion within the MSZW close to the solubility curve where the secondary nucleation rate is minimal. Combining the knowledge of this subregion with seeded experiments with relatively few seeds in the form of coarse crystals from the previous batch would lead to better control capabilities. Using few product crystals as seeds improves the descriptive capacity of the secondary nucleation model (Gahn and Mersmann)[43] as they form a system as described in the model of parent crystals giving rise to attrition fragments.[44]

6. CONCLUSIONS

A rapid strategy for crystallization process development has been presented and demonstrated for ADD-NEOP using PAT tools at both lab scale and industrial scale. Integration of a number of PAT tools into a measurement skid which can be coupled to an existing crystallizer via a circulation flow allows for a flexible application of the PAT tools. The skid also circumvents the time- and cost-intensive design modifications which are conventionally necessary to incorporate PAT tools at industrial scale. The presented process development strategy allowed for collection of thermodynamic and kinetic information at industrial scale without much *a priori* knowledge. Monitoring of the process variables with the help of PAT tools enabled obtaining valuable process insights which can be used to optimize the process. This strategy of process development can also be combined with different control strategies to obtain better control over the product quality.

AUTHOR INFORMATION

Corresponding Author

*s.s.kadam@tudelft.nl

Notes

The authors declare no competing financial interest.

ACKNOWLEDGMENTS

We thank MSD for allowing the experimental campaign at their Oss and Apeldoorn sites in The Netherlands. We also thank Ramon Harting, Edwin Stokkingreef, Frido Roloff, William de Wildt, and Ger van der Veen for the help with experiments during the campaign. The Institute for Sustainable Process

Technology (ISPT) is gratefully acknowledged for financial support.

REFERENCES

(1) Mullin, J. W. *Crystallization*, 4rth ed.; Butterworth-Heinemann: Oxford, 2001.

(2) Rohani, S.; Horne, S.; Murthy, K. Control of Product Quality in Batch Crystallization of Pharmaceuticals and Fine Chemicals. Part 1: Design of the Crystallization Process and the Effect of Solvent. *Org. Process Res. Dev.* **2005**, *9* (6), 858−872.

(3) Birch, M.; Fussell, S. J.; Higginson, P. D.; McDowall, N.; Marziano, I. Towards a PAT-Based Strategy for Crystallization Development. *Org. Process Res. Dev.* **2005**, *9* (3), 360−364.

(4) Black, S. N.; Quigley, K.; Parker, A. A Well-Behaved Crystallisation of a Pharmaceutical Compound. *Org. Process Res. Dev.* **2006**, *10* (2), 241−244.

(5) Kougoulos, E.; Jones, A. G.; Wood-Kaczmar, M. W. A Hybrid CFD Compartmentalization Modeling Framework for the Scaleup of Batch Cooling Crystallization Processes. *Chem. Eng. Commun.* **2006**, *193* (8), 1008−1023.

(6) Myerson, A. S. *Handbook of Industrial Crystallization*, 2nd ed.; Butterworth-Heinemann: Woburn, MA, 2002.

(7) Prausnitz, J. M. L., R. N.; Azevedo, E. G. *Molecular Thermodynamics of Fluid-phase Equilibria*; Prentice-Hall: New Jersey, 1999.

(8) Fredenslund, A.; Jones, R. L.; Prausnitz, J. M. Group-contribution estimation of activity coefficients in nonideal liquid mixtures. *AIChE J.* **1975**, *21* (6), 1086−1099.

(9) Eckert, F.; Klamt, A. Fast solvent screening via quantum chemistry: COSMO-RS approach. *AIChE J.* **2002**, *48* (2), 369−385.

(10) Tung, H.-H.; Tabora, J.; Variankaval, N.; Bakken, D.; Chen, C.-C. Prediction of pharmaceutical solubility Via NRTL-SAC and COSMO-SAC. *J. Pharm. Sci.* **2008**, *97* (5), 1813−1820.

(11) Lee, A. Y.; Erdemir, D.; Myerson, A. S. Crystal Polymorphism in Chemical Process Development. *Annu. Rev. Chem. Biomol. Eng.* **2011**, *2* (1), 259−280.

(12) Kulkarni, S. A.; McGarrity, E. S.; Meekes, H.; ter Horst, J. H., Isonicotinamide self-association: the link between solvent and polymorph nucleation. *Chem. Commun.* **2012**.

(13) Anderton, C. A Valuable Technique for Polymorph Screening. *Eur. Pharm. Rev.* **2004**, 68−74.

(14) Cui, Y.; Yao, E. Evaluation of hydrate-screening methods. *J. Pharm. Sci.* **2008**, *97* (7), 2730−2744.

(15) Jaroslav, N. Kinetics of nucleation in solutions. *J. Cryst. Growth* **1968**, *3*−*4*, 377−383.

(16) Kadam, S. S.; Kulkarni, S. A.; Coloma Ribera, R.; Stankiewicz, A. I.; ter Horst, J. H.; Kramer, H. J. M. A new view on the metastable zone width during cooling crystallization. *Chem. Eng. Sci.* **2012**, *72*, 10−19.

(17) Jiang, S.; ter Horst, J. H. Crystal Nucleation Rates from Probability Distributions of Induction Times. *Cryst. Growth Des.* **2010**, *11* (1), 256−261.

(18) Christiansen, J. A.; Nielsen, A. E. On the Kinetics of Formation of Precipitates of Sparingly Soluble Salts. *Acta Chem. Scand.* **1951**, 673−674.

(19) Galkin, O.; Vekilov, P. G. Direct Determination of the Nucleation Rates of Protein Crystals. *J. Phys. Chem. B* **1999**, *103* (49), 10965−10971.

(20) Hengstermann, A.; Kadam, S.; Jansens, P. J. Influence of Supercooling and Water Content on Crystal Morphology of Acrylic Acid. *Cryst. Growth Des.* **2009**, *9* (4), 2000−2007.

(21) Kadam, S. S.; Mesbah, A.; van der Windt, E.; Kramer, H. J. M. Rapid online calibration for ATR-FTIR spectroscopy during batch crystallization of ammonium sulphate in a semi-industrial scale crystallizer. *Chem. Eng. Res. Des.* **2011**, *89* (7), 995−1005.

(22) Zhang, Y.; Doherty, M. F. Simultaneous prediction of crystal shape and size for solution crystallization. *AIChE J.* **2004**, *50* (9), 2101−2112.

(23) Glade, H.; Ilyaskarov, A. M.; Ulrich, J. Determination of Crystal Growth Kinetics Using Ultrasonic Technique. *Chem. Eng. Technol.* **2004**, *27* (7), 736−740.

(24) Chung, S. H.; Ma, D. L.; Braatz, R. D. Optimal seeding in batch crystallization. *Can. J. Chem. Eng.* **1999**, *77* (3), 590−596.

(25) Bakar, M. R. A.; Nagy, Z. K.; Rielly, C. D. Seeded Batch Cooling Crystallization with Temperature Cycling for the Control of Size Uniformity and Polymorphic Purity of Sulfathiazole Crystals. *Org. Process Res. Dev.* **2009**, *13* (6), 1343−1356.

(26) Jones, A. G. *Crystallization Process Systems*; Butterworth-Heinemann: Oxford, 2002.

(27) Mesbah, A.; Huesman, A. E. M.; Kramer, H. J. M.; Nagy, Z. K.; Van den Hof, P. M. J. Real-time control of a semi-industrial fed-batch evaporative crystallizer using different direct optimization strategies. *AIChE J.* **2011**, *57* (6), 1557−1569.

(28) Zoltan, K, N. Model based robust control approach for batch crystallization product design. *Comput. Chem. Eng.* **2009**, *33* (10), 1685−1691.

(29) Richard, D, B. Advanced control of crystallization processes. *Annu. Rev. Control* **2002**, *26* (1), 87−99.

(30) Kadam, S. S.; Kramer, H. J. M.; ter Horst, J. H. Combination of a Single Primary Nucleation Event and Secondary Nucleation in Crystallization Processes. *Cryst. Growth Des.* **2011**, *11* (4), 1271−1277.

(31) Rozsa, L. SeedMaster 2: A Universal Crystallization Transmitter and Automatic Seeding Device. *Int. Sugar J.* **2006**, *108* (1296), 683−695.

(32) Challis, R. E.; Povery, M. J. W.; Mather, M. L.; Holmes, A. K. Ultrasound Techniques for Characterizing Colloidal Particles. *Rep. Prog. Phys.* **2005**, *68* (7), 1541−1637.

(33) Kadam, S. S.; van der Windt, E.; Daudey, P. J.; Kramer, H. J. M. A Comparative Study of ATR-FTIR and FT-NIR Spectroscopy for In-Situ Concentration Monitoring during Batch Cooling Crystallization Processes. *Cryst. Growth Des.* **2010**, *10* (6), 2629−2640.

(34) Li, R. F.; Penchev, R.; Ramachandran, V.; Roberts, K. J.; Wang, X. Z.; Tweedie, R. J.; Prior, A.; Gerritsen, J. W.; Hugen, F. M. Particle Shape Characterisation via Image Analysis: from Laboratory Studies to In-process Measurements Using an in Situ Particle Viewer System. *Org. Process Res. Dev.* **2008**, *12* (5), 837−849.

(35) ADD-NEOP absolute stereochemistry, obtained from SciFinder Scholar (accessed on 24th September 2010).

(36) Simon, L. L.; Nagy, Z. K.; Hungerbuhler, K. Comparison of external bulk video imaging with focused beam reflectance measurement and ultra-violet visible spectroscopy for metastable zone identification in food and pharmaceutical crystallization processes. *Chem. Eng. Sci.* **2009**, *64* (14), 3344−3351.

(37) Dunuwila, D. D.; Berglund, K. A. ATR-FTIR spectroscopy for in situ measurement of supersaturation. *J. Cryst. Growth* **1997**, *179* (1−2), 185−193.

(38) Brown, S. D.; Sum, S. T.; Despagne, F.; Lavine, B. K. Chemometrics. *Anal. Chem.* **1996**, *68* (12), 21−62.

(39) Bjørsvik, H.-R. Online Spectroscopy and Multivariate Data Analysis as a Combined Tool for Process Monitoring and Reaction Optimization. *Org. Process Res. Dev.* **2004**, *8* (3), 495−503.

(40) Aamir, E.; Nagy, Z. K.; Rielly, C. D. Optimal seed recipe design for crystal size distribution control for batch cooling crystallisation processes. *Chem. Eng. Sci.* **2010**, *65* (11), 3602−3614.

(41) Nagy, Z. K.; Fujiwara, M.; Woo, X. Y.; Braatz, R. D. Determination of the Kinetic Parameters for the Crystallization of Paracetamol from Water Using Metastable Zone Width Experiments. *Ind. Eng. Chem. Res.* **2008**, *47* (4), 1245−1252.

(42) Daudey, P. J.; van Rosmalen, G. M.; de Jong, E. J. Secondary nucleation kinetcs of ammonium sulfate in a CMSMPR crystallizer. *J. Cryst. Growth* **1990**, *99* (1−4, Part 2), 1076−1081.

(43) Gahn, C.; Mersmann, A. Brittle fracture in crystallization processes Part A. Attrition and abrasion of brittle solids. *Chem. Eng. Sci.* **1999**, *54* (9), 1273−1282.

(44) Kalbasenka, A.; Huesman, A.; Kramer, H. Modeling batch crystallization processes: Assumption verification and improvement of

the parameter estimation quality through empirical experiment design. *Chem. Eng. Sci.* **2011**, *66* (20), 4867−4877.